Higher excited states of acceptors in cubic semiconductors

M. Said, M. A. Kanehisa, and M. Balkanski
Laboratoire de Physique des Solides, Université Pierre et Marie Curie, Tour 13, 4 place Jussieu, 75252 Paris Cédex 05, France

Y. Saad
Research Center for Computation, Yale University, P.O. Box 2158, Yale Station, New Haven, Connecticut 06520
(Received 22 July 1986)

For the first time, higher excited states of shallow acceptors up to the $8S$ and $5P$ states are calculated, using a method based on the Baldereschi-Lipari theory including the cubic correction. The eigenvalues and eigenvectors of the effective-mass Hamiltonian for shallow acceptor states were obtained by the finite-element method. The resulting sparse matrix is diagonalized by a newly developed method based on Arnoldi's algorithm. Except for the lowest n, each hydrogenlike state nL splits into two levels when spherical "spin-orbit" coupling increases from 0 to 1. This results in crossing and repulsion of levels with different n. The spectra are thus shown to have totally different structure in the real acceptor regime $\mu \sim 0.6$ in contrast to exciton spectra for which $\mu \sim 0.1$. The calculated spectra are in agreement with available experimental data, especially in the case of higher excited states for which central-cell correction is negligible. The spectra of the shallow acceptors in ZnTe, CdTe, and InP are calculated and compared with the experimental ones.

I. INTRODUCTION

The effective-mass approximation for shallow impurity states is well established since more than 35 years ago. In the case of donors associated with spherical conduction-band minimum, the spectra are hydrogenlike series and this is well tested by experiments.[1,2] In the case of acceptors, the degeneracy of the valence band prevents an analytical solution of the effective-mass equation, and one has recourse to variational methods, which give only the ground-state, and at best, a few low-lying excited states. Baldereschi and Lipari[3,4] have proposed a new approach to the acceptor problem. They split the Luttinger Hamiltonian into two terms, one of spherical symmetry and the other of cubic symmetry, and show that in most cubic semiconductors, the spherical term is dominant and the cubic term can be considered as a perturbation. Though their approach allows a systematic classification of acceptor states, the coupled radial differential equations are to be solved variationally, and this suffers the same shortcoming as the older tour de force variational methods.

Recently we have succeeded in solving the Balderschi and Lipari radial equation nonvariationally. Our approach is based on the finite-element method and Arnoldi's algorithm for diagonalizing resultant sparse matrices and allows one to obtain simultaneously several eigenvalues and eigenvectors. The method of resolution, together with the numerical solution of the Hamiltonians described in Sec. II are presented in Sec. III. The acceptor Hamiltonian and the radial equations which describe acceptor states of various symmetries are presented in Sec. II. In Sec. IV we compare our results with the experimental ones. This leads to an interesting discussion: Around typical values of μ for which the crossing of levels are forbidden, the corresponding acceptor wave functions are very different from hydrogenic wave functions. In Sec. V we discuss some possible extensions and summarize main results. For convenience, we give in the Appendix the mathematical detail of the method that we have used to diagonalize the sparse matrices.

II. ACCEPTOR HAMILTONIAN

According to Baldereschi and Lipari, in the diamond and zinc-blende structure, the acceptor Hamiltonian in the effective-mass approximation is written as the sum of a spherical term and a cubic correction[3]

$$H = H_s + \mu H_{d,\mathrm{sph}} + \delta H_{d,\mathrm{cub}} \,. \tag{1}$$

Here

$$H_s = \frac{P^2}{\hbar^2} - \frac{2}{r}, \quad H_{d,\mathrm{sph}} = -\frac{1}{9\hbar^2}(\mathbf{P}^{(2)}\cdot\mathbf{J}^{(2)}) \tag{2}$$

are the spherical terms in the notation of Baldereschi and Lipari and

$$H_{d,\mathrm{cub}} = \frac{1}{9\hbar^2}[\mathbf{P}^{(2)}\times\mathbf{J}^{(2)}]^{(4)}_{-4} + \tfrac{1}{5}\sqrt{70}[\mathbf{P}^{(2)}\times\mathbf{J}^{(2)}]^{4}_{0} + [\mathbf{P}^{(2)}\times\mathbf{J}^{(2)}]^{(4)}_{4} \tag{3}$$

is the cubic term with

$$\mu = (6\gamma_3 + 4\gamma_2)/5\gamma_1, \quad \delta = (\gamma_3 - \gamma_2)/\gamma_1 \,. \tag{4}$$

In (1), μ is the strength of the spherical spin-orbit interaction and δ measures the cubic contribution. Energy and length are expressed in units of effective rydberg R_0 and Bohr radius a_0,

$$R_0=\frac{e^4 m_0}{2\hbar^2\epsilon_0^2\gamma_1}\ , \tag{5}$$

$$a_0=\frac{\hbar^2\epsilon_0\gamma_1}{e^2 m_0}\ . \tag{6}$$

This formulation yields a meaningful classification of the acceptor states and reduces the eigenvalue problem to simple radial equations. If we limit our study to the acceptor states with $L=0$ and $L=1$, only the $P_{5/2}$ states are affected by the first-order cubic coupling.[4] As a result we find the following systems of differential equations for the radial wave functions $f(r)$ and $g(r)$:

$$\begin{bmatrix} \frac{d^2}{dr^2}+\frac{2}{r}\frac{d}{dr}+\frac{2}{r^2}+\frac{2}{r}-E & -\mu\left[\frac{d^2}{dr^2}+\frac{5}{r}\frac{d}{dr}+\frac{3}{r^2}\right] \\ -\mu\left[\frac{d^2}{dr^2}-\frac{1}{r}\frac{d}{dr}\right] & \frac{d^2}{dr^2}+\frac{2}{r}\frac{d}{dr}-\frac{6}{r^2}+\frac{2}{r}-E \end{bmatrix}\begin{bmatrix} f(r) \\ g(r)\end{bmatrix}=0\ , \tag{7}$$

for $S_{3/2}$ states. For P_F states ($F=\frac{3}{2},\frac{5}{2}$), one has

$$\begin{bmatrix} a_F\left[\frac{d^2}{dr^2}+\frac{2}{r}\frac{d}{dr}+\frac{2}{r^2}\right]+\frac{2}{r}-E & -c_F\left[\frac{d^2}{dr^2}+\frac{7}{r}\frac{d}{dr}+\frac{8}{r^2}\right] \\ -c_F\left[\frac{d^2}{dr^2}+\frac{3}{r}\frac{d}{dr}+\frac{3}{r^2}\right] & b_F\left[\frac{d^2}{dr^2}+\frac{3}{r}\frac{d}{dr}+\frac{12}{r^2}\right]+\frac{2}{r}-E \end{bmatrix}\begin{bmatrix} f(r) \\ g(r)\end{bmatrix}=0\ . \tag{8}$$

where (a_F,b_F,c_F) are $(1-\frac{4}{5}\mu,\ 1+\frac{4}{5}\mu,\ \frac{3}{5}\mu)$ for $P_{3/2}$, and $(1+\frac{1}{5}\mu+(24/25)\delta,\ 1-\frac{1}{5}\mu-(68/175)\delta,\ (2\sqrt{6}/5)(\mu-\frac{1}{5}\delta))$ for $P_{5/2}(\Gamma_7)$, finally, $(1+\frac{1}{5}\mu-(12/25)\delta,\ 1-\frac{1}{5}\mu+(34/175)\delta,\ (\sqrt{6}/5)(2\mu+\frac{1}{5}\delta))$ for $P_{5/2}(\Gamma_8)$.

Following Baldereschi and Lipari, we shall consider the coupling between the $P_{3/2}(\Gamma_8)$ and $P_{5/2}(\Gamma_8)$, one obtains the radial Hamiltonian,[4]

$$\underline{H}_c=\begin{bmatrix} \underline{H}(\frac{3}{2}) & \sqrt{6}\underline{X} \\ \sqrt{6}X^\dagger & \underline{H}(\frac{5}{2},\Gamma_8)\end{bmatrix}\ , \tag{9}$$

where $H(\frac{3}{2})$ is the Hamiltonian for $P_{3/2}$ and $H(\frac{5}{2},\Gamma_8)$ is the Hamiltonian for $P_{5/2}(\Gamma_8)$ given by (8), and the coupling matrix X is

$$\underline{X}=\begin{bmatrix} \frac{2\sqrt{6}}{25}\delta\left[\frac{d^2}{dr^2}+\frac{2}{r}\frac{d}{dr}-\frac{2}{r^2}\right] & -\frac{18}{175}\delta\left[\frac{d^2}{dr^2}+\frac{7}{r}\frac{d}{dr}+\frac{8}{r^2}\right] \\ -\frac{2\sqrt{6}}{175}\delta\left[\frac{d^2}{dr^2}+\frac{3}{r}\frac{d}{dr}+\frac{3}{r^2}\right] & \frac{22}{175}\delta\left[\frac{d^2}{dr^2}+\frac{2}{r}\frac{d}{dr}-\frac{12}{r^2}\right]\end{bmatrix}\ . \tag{10}$$

Until now, these equations have been solved only by variational methods and only $1S$, $2S$, and $2P$ states have been calculated. Before going into the numerical solution of Eqs. (7), (8), and (9), we shall examine the properties of coupled equations using the perturbation theory. Beyond $n=2$ (where n is the usual hydrogenic principal quantum number), Eq. (7) gives for $\mu=0$ degenerate hydrogenous states ($3S$,$3D$), ($4S$,$4D$), etc. For $\mu\neq 0$ these states split into two states each, that we write for small values of μ in the form $\phi_{a,b}=A\phi_s\pm B\phi_d$, where ϕ_s and ϕ_d are the S and D degenerate initial hydrogenic functions. A and B are given by

$$A=\frac{(V_1)^{1/2}}{(V_1+V_2)^{1/2}}\quad\text{and}\quad B=\frac{(V_2)^{1/2}}{(V_1+V_2)^{1/2}}\ , \tag{11}$$

where

$$V_1=-\mu\left\langle\phi_s\left|\frac{d^2}{dr^2}+\frac{5}{r}\frac{d}{dr}+\frac{3}{r^2}\right|\phi_d\right\rangle$$

and

$$V_2=-\mu\left\langle\phi_d\left|\frac{d^2}{dr^2}+\frac{5}{r}\frac{d}{dr}+\frac{3}{r^2}\right|\phi_s\right\rangle\ .$$

The corresponding energies are $E_{a,b}=E_0\pm\mu\sqrt{(V_1V_2)}$. As a result, we find for $n=3$, $E_{a,b}=\frac{1}{9}(1\pm 1/\sqrt{10})$ and $A=B=1/\sqrt{2}$. We shall denote, hereafter, the upper levels associated with E_a and which are of "bonding" character, by $S_{3/2a}$. The lower ones, associated with E_b and which are of "antibonding" character, will be denoted by $S_{3/2b}$. Note that E_a increase and E_b decrease when μ increases; this result will be exploited in the following sec-

tions. The above Hamiltonian will be numerically solved in Sec. III.

III. METHOD OF SOLUTION AND RESULT

Up to now, there was no systematic method to calculate higher excited states of (7), (8), and (9), only variational methods[3,4] which give the lowest states, or a coarse empirical relationship[5] have been employed. We shall solve the coupled radial equations by the finite-element method.[6] The same method was used by Mattausch and Uihlein[7] to calculate the fine structure of P excitons in CuBr. The main idea of the finite-element method is to approximate the differential operators occurring in the eigenvalue equations by finite difference expressions using the values of the wave function at neighboring equidistant points. For this purpose the argument of the radial functions is regarded as a discrete variable running through equidistant points within an interval given by the origin and a cutoff radius. The origin has to be excluded as one of the discrete values of the variable r, because of the singularities of the differential equations occurring there. We restrict ourselves to the first-order term in the development of the differential operators. Then the differential operator

$$D_{LL'}=\frac{d^2}{dr^2}+\frac{a_{LL'}}{r}\frac{d}{dr}+\frac{b_{LL'}}{r^2}\ ,$$

where, for $L,L'=0,2$,

$$a_{LL'}=\begin{bmatrix}2 & 5\\ -1 & 2\end{bmatrix},\quad b_{LL'}=\begin{bmatrix}0 & 3\\ 0 & -6\end{bmatrix}$$

and for $L,L'=1,3$,

$$a_{LL'}=\begin{bmatrix}2 & 7\\ -3 & 2\end{bmatrix},\quad b_{LL'}=\begin{bmatrix}-2 & 8\\ 3 & -12\end{bmatrix}$$

are now replaced by the $n\times n$ matrix approximating $D_{LL'}$ which is given by

$$(D_{LL'})_{i,i'}=\frac{1}{h^2}(\delta_{i,i'-1}+\delta_{i,i'+1}-2\delta_{i,i'})+\frac{a_{LL'}}{2r_i h}(\delta_{i,i'-1}-\delta_{i,i'+1})+\frac{b_{ll'}}{r_i^2}\delta_{i,i'}\ .$$

Here h is the distance between the points. The choice of the number of points n and the cutoff radius depends on the state to be computed. As an example, to compute $5P_{5/2}(\Gamma_8)$ we take the cutoff radius value $70a_0$.

In order to diagonalize the resulting matrix, we use Arnoldi's method.[8] The principle of this method is the following. To compute the desired eigenvalues and eigenvectors of our $n\times n$ matrix, we begin by constructing a basis of dimension $m\ll n$; we project our matrix on this basis and we obtain a $\underline{H}_m$ matrix. The diagonalization of $\underline{H}_m$ gives the desired eigenvalues and eigenvectors. The detail of this method is explained in the Appendix.

In typical cases, to compute 12 eigenvalues and their eigenvectors, it takes about 3 min on a NAS 9080 computer. We have checked that the n^{-2} law is satisfied for the hydrogen case ($\mu=0, \delta=0$). Degenerate states are correctly calculated. A good agreement has been obtained for small μ ($0<\mu<0.06$) between numerical solutions and the perturbation theory, as shown in Fig. 1. For all μ we obtain good agreement in $1S$, $2S$, and $2P$ states with Baldereschi and Lipari.[3,4]

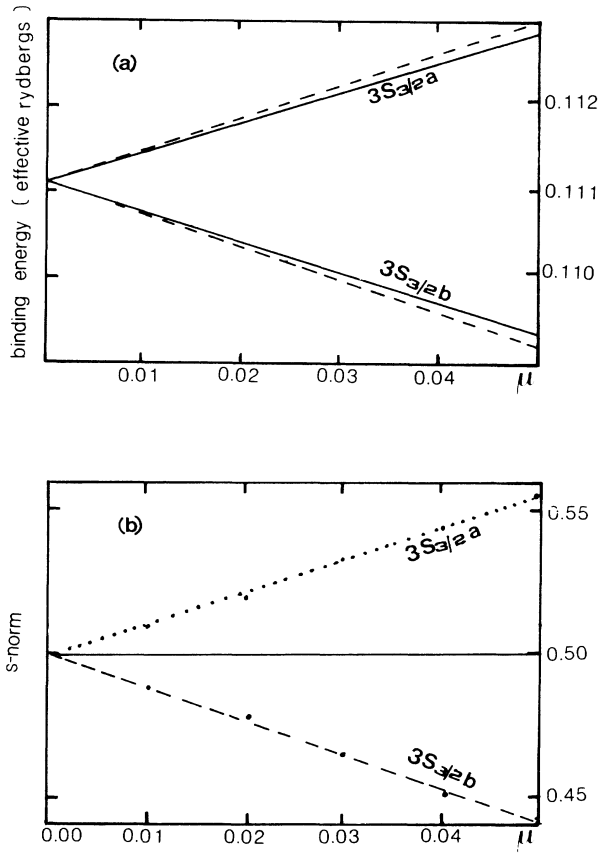

FIG. 1. (a) Calculated $3S_{3/2a}$ and $3S_{3/2b}$ energies using the numerical method (solid curve) and perturbation method theory (dashed curve). The energies are in units of the effective rydberg R_0. (b) s-norm contribution to the $3S_{3/2a}$, and $3S_{3/2b}$ eigenvectors using perturbation theory (solid curve) and numerical results, dotted curve for $3S_{3/2a}$ and dashed curve for $3S_{3/2b}$.

TABLE I. Energies of the first eight $S_{3/2}$ acceptor states as functions of the parameter μ. The energies are in units of the effective rydberg R_0. Because of the level crossing for larger μ (see Fig. 2), the entries are presented here in order of decreasing energy.

μ	1	2	3	4	5	6	7	8
0.00	0.9998	0.2500	0.1111	0.1111	0.0624	0.0624	0.0397	0.0394
0.05	1.0021	0.2509	0.1131	0.1095	0.0640	0.0611	0.0409	0.0383
0.10	1.0089	0.2535	0.1156	0.1081	0.0658	0.0598	0.0424	0.0371
0.15	1.0205	0.2580	0.1189	0.1069	0.0681	0.0586	0.0441	0.0356
0.20	1.0372	0.2644	0.1231	0.1056	0.0709	0.0574	0.0461	0.0356
0.25	1.0596	0.2728	0.1282	0.1042	0.0743	0.0561	0.0471	0.0414
0.30	1.0886	0.2835	0.1345	0.1028	0.0784	0.0548	0.0507	0.0411
0.35	1.1250	0.2968	0.1421	0.1013	0.0832	0.0544	0.0534	0.0415
0.40	1.1706	0.3131	0.1521	0.0999	0.0890	0.0585	0.0520	0.0423
0.45	1.2274	0.3331	0.1623	0.0986	0.0958	0.0633	0.0507	0.0433
0.50	1.2984	0.3558	0.1758	0.1047	0.0967	0.0691	0.0516	0.0483
0.55	1.3800	0.3880	0.1924	0.1150	0.0953	0.0760	0.0549	0.0490
0.60	1.5029	0.4265	0.2132	0.1281	0.0944	0.0844	0.0611	0.0483
0.65	1.6537	0.4762	0.2400	0.1448	0.0986	0.0902	0.0693	0.0520
0.70	1.8580	0.5426	0.2756	0.1671	0.1128	0.0901	0.0800	0.0602
0.75	2.1478	0.6355	0.3253	0.1981	0.1338	0.0966	0.0880	0.0718
0.80	2.5885	0.7750	0.3992	0.2444	0.1654	0.1192	0.0914	0.0853
0.85	3.3375	1.0082	0.5218	0.3208	0.2177	0.1572	0.1189	0.0934
0.90	4.9091	1.4830	0.7669	0.4726	0.3216	0.2328	0.1764	0.1381
0.95	10.122	2.9142	1.4713	0.9060	0.6179	0.4491	0.3414	0.2682

The energies of the first eight $S_{3/2}$ states are given in Table I as a function of μ. Figure 2 shows the energy spectra of these states except for the ground state $1S_{3/2}$ already reported by Baldereschi and Lipari.[3] We can see from this diagram that, except for $n=2$, each hydrogen-like state nL splits into two levels ($S_{3/2a}, S_{3/2b}$) when spherical "spin-orbit" coupling increases from 0 to 1, and

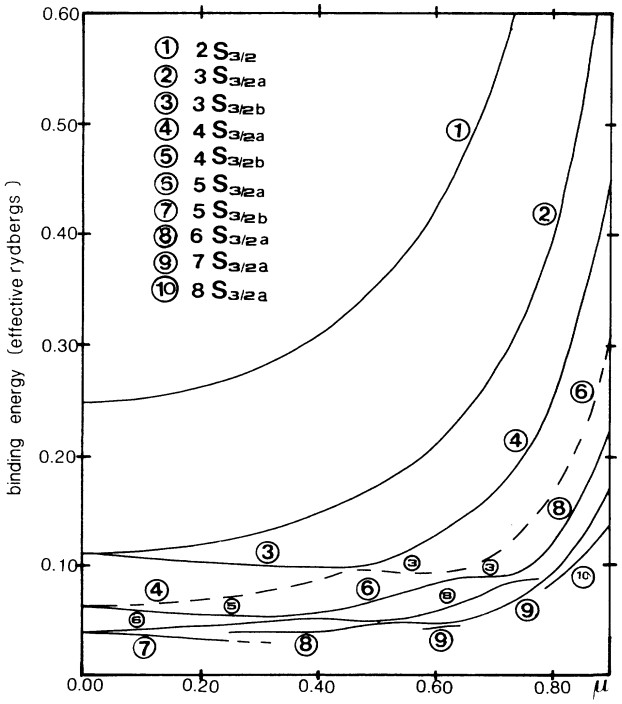

FIG. 2. Calculated acceptor energy spectrum of $nS_{3/2}$ ($n=2,3,\ldots,8$) states as function of the parameter μ. The energies are in units of the effective rydberg R_0.

the $nS_{3/2a}$ states increase with μ while the $nS_{3/2b}$ decrease with increasing μ. This gives rise to the possibility of level crossing, but these crossings are forbidden because the states have the same symmetry. This leads to a totally different structure of the spectra in the real acceptor regime $\mu \approx 0.6$ in contrast to exciton spectra for which $\mu \approx 0.1$. It is also clear from Fig. 2 that, if we always consider the first eight states, then for $\mu < 0.20$, three states (the $3S_{3/2b}$, $4S_{3/2b}$, and $5S_{3/2b}$ states) are of antibonding character. For $0.20 < \mu < 0.68$, only two states remain with antibonding character (the $3S_{3/2b}$ and $4S_{3/2b}$ states), while for $0.68 < \mu < 0.86$, only the $3S_{3/2b}$ state is left with antibonding character. For $\mu > 0.86$ all the first eight states are of bonding character. One should note, however, that for the values of μ for which the level repulsion occurs, the wave functions deviate considerably from hydrogenic wave functions. Among the states represented in Fig. 2, let us now consider, for example, those represented by the dashed curve. We can see that, for $\mu < 0.46$, the state represented by this curve is the $4S_{3/2a}$, state, while it becomes the $3S_{3/2b}$ state for $0.46 < \mu < 0.68$, and the $6S_{3/2a}$ state for $\mu > 0.68$. This clearly shows the gradual disappearance of the antibonding character, and proves that μ is an important parameter for determining the nature of the various states and subsequently the transitions associated with them. We have also computed the norm (magnitude) corresponding to each $S_{3/2}$. The contribution to the magnitude coming from $f(r)$ is noted s norm, and the contribution coming from $g(r)$ is noted d norm. The normalization procedure is identical to the one described in Ref. 3. We note that, except for particular values of μ ($\mu \approx 0.45$ and $\mu \approx 0.60$) for which the $5S_{3/2}$ state has a predominantly d character (d norm ≈ 0.9), the difference between the s and d norm (≈ 0.2 or less) for each $S_{3/2}$ state is not sufficient to predict the predominant character of the state.

TABLE II. Energies of the nP ($n=2,3,4,5$) acceptor states as functions of the parameter μ. The cubic coupling parameter is $\delta=0.05$. The energies are in units of the effective rydberg R_0.

μ	$2P_{3/2}(\Gamma_8)$	$2P_{5/2}(\Gamma_8)$	$2P_{5/2}(\Gamma_7)$	$3P_{3/2}(\Gamma_8)$	$3P_{5/2}(\Gamma_8)$	$3P_{5/2}(\Gamma_7)$	$4P_{3/2}(\Gamma_8)$	$4P_{5/2}(\Gamma_8)$	$4P_{5/2}(\Gamma_7)$	$5P_{3/2}(\Gamma_8)$	$5P_{5/2}(\Gamma_8)$	$5P_{5/2}(\Gamma_7)$
0.00	0.2601	0.2464	0.2386	0.1156	0.1095	0.1060	0.0633	0.0623	0.0637	0.0614	0.0571	0.0594
0.05	0.2646	0.2508	0.2367	0.1177	0.1116	0.1053	0.0649	0.0625	0.0644	0.0600	0.0589	0.0590
0.10	0.2749	0.2524	0.2361	0.1223	0.1128	0.1055	0.0682	0.0639	0.0649	0.0595	0.0565	0.0591
0.15	0.2881	0.2542	0.2369	0.1284	0.1144	0.1066	0.0720	0.0656	0.0655	0.0591	0.0527	0.0596
0.20	0.3036	0.2572	0.2391	0.1355	0.1168	0.1087	0.0763	0.0677	0.0664	0.0586	0.0529	0.0603
0.25	0.3215	0.2618	0.2429	0.1437	0.1202	0.1118	0.0812	0.0705	0.0680	0.0578	0.0536	0.0606
0.30	0.3422	0.2684	0.2484	0.1532	0.1247	0.1159	0.0867	0.0739	0.0705	0.0562	0.0551	0.0605
0.35	0.3664	0.2771	0.2558	0.1642	0.1303	0.1211	0.0931	0.0780	0.0740	0.0574	0.0522	0.0600
0.40	0.3948	0.2885	0.2656	0.1772	0.1374	0.1275	0.1005	0.0830	0.0784	0.0638	0.0571	0.0595
0.45	0.4285	0.3032	0.2783	0.1926	0.1462	0.1353	0.1094	0.0891	0.0837	0.0701	0.0602	0.0593
0.50	0.4692	0.3221	0.2946	0.2111	0.1571	0.1540	0.1200	0.0964	0.0902	0.0773	0.0647	0.0619
0.55	0.5190	0.3465	0.3155	0.2338	0.1708	0.1570	0.1330	0.1054	0.0981	0.0858	0.0712	0.0673
0.60	0.5815	0.3784	0.3425	0.2623	0.1883	0.1721	0.1493	0.1168	0.1080	0.0964	0.0796	0.0744
0.65	0.6621	0.4210	0.3781	0.2989	0.2111	0.1915	0.1703	0.1316	0.1206	0.1100	0.0902	0.0833
0.70	0.7698	0.4795	0.4262	0.3478	0.2422	0.2174	0.1983	0.1514	0.1372	0.1282	0.1042	0.0951
0.75	0.9210	0.5637	0.4937	0.4164	0.2864	0.2533	0.2376	0.1794	0.1601	0.1537	0.1237	0.1111
0.80	1.1485	0.6937	0.5939	0.5196	0.3541	0.3061	0.2966	0.2220	0.1937	0.1920	0.1532	0.1345
0.85	1.5299	0.9171	0.7559	0.6925	0.4698	0.3910	0.3956	0.2945	0.2474	0.2563	0.2033	0.1719
0.90	2.3021	1.3842	1.0589	1.0418	0.7095	0.5490	0.5956	0.4440	0.3470	0.3867	0.3058	0.2410
0.95	4.6951	2.8542	1.8114	2.1084	1.4344	0.9359	1.2084	0.8886	0.5901	0.7914	0.6084	0.4094

TABLE III. Same as Table II but the cubic coupling parameter is $\delta=0.15$. The energies are in units of the effective rydberg R_0.

μ	$2P_{3/2}(\Gamma_8)$	$2P_{5/2}(\Gamma_8)$	$2P_{5/2}(\Gamma_7)$	$3P_{3/2}(\Gamma_8)$	$3P_{5/2}(\Gamma_8)$	$3P_{5/2}(\Gamma_7)$	$4P_{3/2}(\Gamma_8)$	$4P_{5/2}(\Gamma_8)$	$4P_{5/2}(\Gamma_7)$	$5P_{3/2}(\Gamma_8)$	$5P_{5/2}(\Gamma_8)$	$5P_{5/2}(\Gamma_7)$
0.00	0.2830	0.2400	0.2187	0.1258	0.1066	0.0973	0.0708	0.0629	0.0663	0.0606	0.0596	0.0541
0.05	0.2856	0.2462	0.2167	0.1270	0.1097	0.0964	0.0714	0.0624	0.0671	0.0612	0.0592	0.0534
0.10	0.2917	0.2521	0.2159	0.1299	0.1128	0.0964	0.0732	0.0644	0.0675	0.0610	0.0573	0.0537
0.15	0.3016	0.2577	0.2163	0.1344	0.1160	0.0974	0.0757	0.0667	0.0677	0.0607	0.0552	0.0547
0.20	0.3148	0.2634	0.2179	0.1406	0.1196	0.0994	0.0794	0.0694	0.0677	0.0603	0.0532	0.0562
0.25	0.3314	0.2702	0.2209	0.1482	0.1238	0.1023	0.0839	0.0725	0.0679	0.0599	0.0537	0.0579
0.30	0.3515	0.2784	0.2255	0.1574	0.1290	0.1061	0.0893	0.0759	0.0688	0.0593	0.0573	0.0592
0.35	0.3754	0.2887	0.2317	0.1684	0.1353	0.1109	0.0956	0.0804	0.0708	0.0616	0.0587	0.0598
0.40	0.4039	0.3018	0.2400	0.1815	0.1431	0.1167	0.1031	0.0859	0.0741	0.0666	0.0586	0.0598
0.45	0.4381	0.3183	0.2507	0.1971	0.1526	0.1237	0.1122	0.0922	0.0785	0.0722	0.0614	0.0595
0.50	0.4796	0.3393	0.2644	0.2161	0.1645	0.1321	0.1231	0.1001	0.0840	0.0795	0.0667	0.0598
0.55	0.5309	0.3665	0.2819	0.2396	0.1794	0.1425	0.1367	0.1098	0.0908	0.0885	0.0738	0.0631
0.60	0.5957	0.4021	0.3044	0.2692	0.1985	0.1553	0.1537	0.1221	0.0992	0.0997	0.0827	0.0689
0.65	0.6800	0.4497	0.3336	0.3076	0.2237	0.1715	0.1760	0.1380	0.1098	0.1143	0.0939	0.0765
0.70	0.7940	0.5159	0.3723	0.3597	0.2583	0.1926	0.2061	0.1597	0.1234	0.1341	0.1087	0.0862
0.75	0.9569	0.6124	0.4252	0.4343	0.3081	0.2212	0.2494	0.1906	0.1417	0.1627	0.1299	0.0991
0.80	1.2103	0.7640	0.5008	0.5505	0.3855	0.2616	0.3170	0.2381	0.1675	0.2076	0.1619	0.1173
0.85	1.6641	1.0310	0.6164	0.7595	0.5205	0.3230	0.4393	0.3200	0.2066	0.2890	0.2167	0.1446
0.90	2.7575	1.6035	0.8126	1.2595	0.8131	0.4269	0.7255	0.5090	0.2726	0.4676	0.3573	0.1905
0.95	12.708	4.9232	1.2142	3.1077	2.5680	0.6382	1.7219	1.5097	0.4066	1.2184	1.0000	0.2837

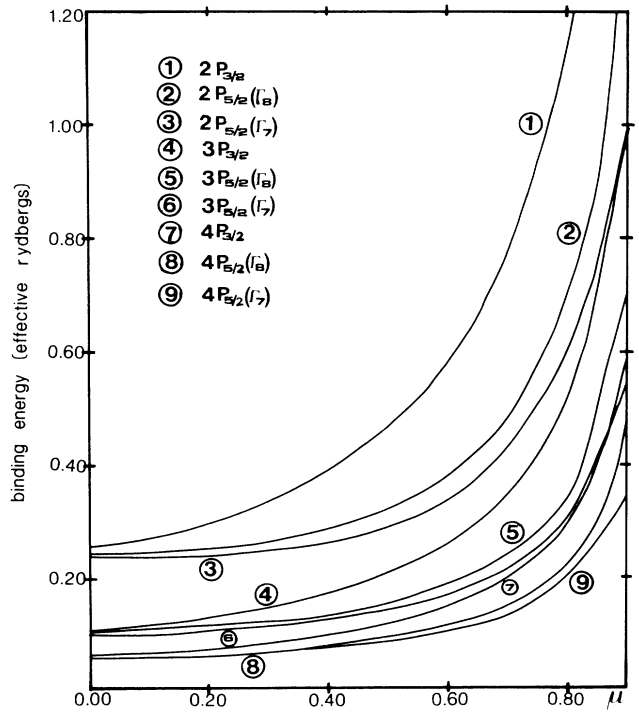

FIG. 3. Calculated acceptor energy spectrum of nP ($n=2,3,\ldots,4$) states as a function of the parameter μ and for a cubic coupling parameter $\delta=0.05$. The energies are in units of the effective rydberg R_0.

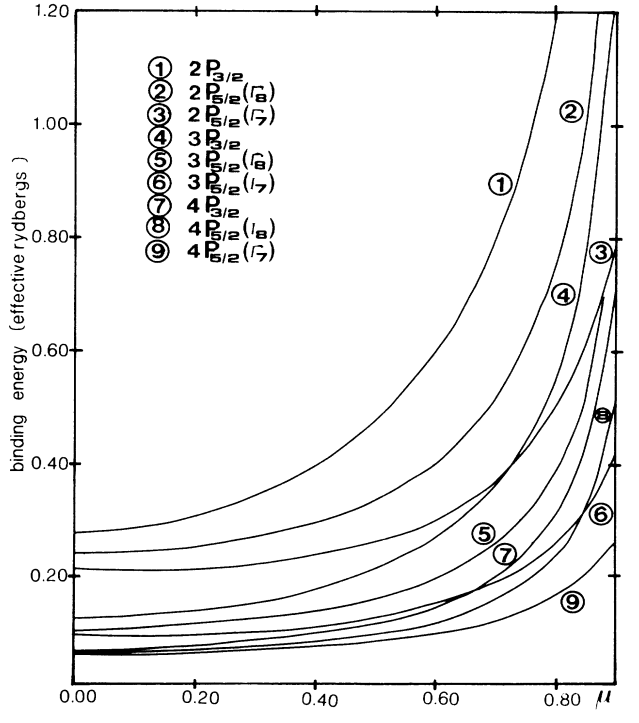

FIG. 4. Same as Fig. 2 but for a cubic coupling parameter $\delta=0.15$. The energies are in units of the effective rydberg R_0.

So much for the S states. Let us now turn our attention to the P states which, apart from the shallowest three ($n=2$), have not been reported previously either theoretically or experimentally. The energies of the first nP ($n<6$) for typical values of δ ($\delta=0.05$ and $\delta=0.15$) are tabulated as a function of μ in Tables II and III, respectively. The corresponding spectra are given in Figs. 3 and 4. We note that $nP(\Gamma_8)$ increase more rapidly than $nP(\Gamma_7)$ when δ increases; this causes crossings between these states. Unlike the case of the S states, however, crossings here are allowed because of the difference in symmetry. In Fig. 4, the first crossing between $3P_{5/2}(\Gamma_7)$ and $4P_{3/2}(\Gamma_8)$ is for $\mu\approx0.66$, the next between $2P_{5/2}(\Gamma_7)$ and $3P_{3/2}(\Gamma_8)$ is for $\mu\approx0.71$ and another one between $3P_{5/2}(\Gamma_7)$, and $4P_{5/2}(\Gamma_8)$ is for $\mu\approx0.86$. However, there is no crossing in the region ($0.00<\mu<0.86$) in the case of $\delta=0.05$, as is shown in Fig. 3.

IV. COMPARISON WITH EXPERIMENT

In this section, we compare our calculated values with the given experimental ones. A considerable amount of experimental data now exists for acceptor centers in II-VI and III-V compounds, particularly in ZnTe,[9] CdTe,[10] and InP,[11] where luminescence, infrared absorption, and Raman spectroscopy have been used to measure the ground and excited states. Let us focus our attention on Li- and P-doped ZnTe (for which detailed experimental data are available[5,9,12–15]) since it is known experimentally that Li and P are shallow acceptors and hence the influence of the central-cell correction is expected to be negligible for excited states. We have calculated some values of excited states using the values of μ and δ proposed by Venghaus *et al.*[13] ($\mu=0.57,\delta=0.12$), or by Nakashima *et al.*[12] ($\mu=0.61,\delta=0.15$). These values of μ and δ do not lead to a perfect agreement between the measured and the calculated energy values. Better agreement is found if we use the values of μ and δ proposed by Herbert *et al.*[5] ($\mu=0.58,\delta=0.12$). Furthermore, the latter authors have supposed that in p-type ZnTe the $5S_{3/2}$ and the $8S_{3/2}$ states are of predominantly d character. The results of our calculations on the S states do not contradict this supposition, especially since the value of μ ($\mu=0.60$) which we have reported for ZnTe in a previous publication (Ref. 15) falls nicely within the range ($\mu\approx0.45$ and $\mu\approx0.60$) for which we established here that the $5S_{3/2}$ state has considerable d character, but this is not so significant for the $8S_{3/2}$ state for which we found d norm ≈0.65. It is worth noting that this value of μ ($\mu=0.60$) is distinctly different from any value for which level crossings may be encountered.

All the proposed values of μ and δ give the same classification for the acceptor states which were proposed by Venghaus and Dean[9] for ZnTe:As spectra, where phonon and electronic spectra are widely separated. This classification shows that $3S_{3/2}$ is higher than $2P_{5/2}(\Gamma_7)$ and necessitates a reinterpretation of the ZnTe:Li and ZnTe:P spectra given by Nakashima *et al.*[12] The P and As cases show the effect of the central-cell correction that one can isolate by considering the difference between the measured

and the calculated ground-state values. In Table IV we give a comparison between our calculated values and the experimental results of Refs. 5 and 9–13 corresponding to the shallowest acceptor in each case. For the values proposed by Nakashima *et al.*,[12] we compare the experimental and theoretical data to within a constant (3.1 meV $= E_{g,\mathrm{Ven}} - E_{g,\mathrm{Na}}$), where $E_{g,\mathrm{Ven}}$ and $E_{g,\mathrm{Na}}$ are the energy gap of ZnTe proposed by Venghaus and Dean[9] and Nakashima *et al.*,[16] because their experimentally determined energy gap is incorrect.[17] It should be noted that in our calculation we have used the values of μ and δ which were proposed by the authors of the above-mentioned references. In the case of the II-VI compounds we note that, using these proposed values of μ and δ, the agreement between experiment and theory is not very satisfactory. However, in the case of the III-V compounds, such a comparison between theory and experiment for higher acceptor excited states is not as easily possible because such states are known to be difficult to be measured experimentally.

V. CONCLUDING REMARKS

The comparison between our energy levels using the proposed μ and δ values and the experimental ones is satisfactory. However, these parameters are determined only from the few low-lying excited states that are easily affected by the central-cell effect and are therefore approximate. We have shown in the case of ZnTe (Ref. 15) that these values of μ and δ can be determined more accurately if we take into account the higher excited states. This will also apply to other compounds as well. These higher excited states are worthy of further attention.

In Fig. 2 we have shown that some levels may change their character (for example bonding to antibonding) when μ varies. This implies that the corresponding transitions to these levels may or may not be detected. For example, in the case of ZnTe Herbert *et al.*[5] report that they have not seen the transitions corresponding to the $5S_{3/2}$ and $8S_{3/2}$ states because these states are of predominantly d character. Furthermore, it is perhaps worthwhile giving further attention to the study of D states, since we have shown in the case of p-type ZnTe the existence of, for example, a $3D_{5/2}(\Gamma_8)$ state between the $2P_{5/2}(\Gamma_7)$ and $3P_{3/2}$ states (Ref. 14). To our knowledge, such D states have not been treated in the literature. We hope to treat these questions in the near future.

In conclusion, we have shown that excited acceptor states associated with a degenerate valence band can be obtained almost as systematically as donor excited states. Our new approach will allow the exploration of experimental results so far discarded because of the lack of numerical calculations. To make reliable predictions, our comparison between experimental and theoretical data in the case of p-type ZnTe (Ref. 15) leads to new and better Luttinger valence-band parameters γ_1, γ_2, and γ_3 that, up to now, had been given by variational methods. Our method shows that more observed spectra must be reinterpreted with closer attention to higher excited states for which more crossing may or may not be possible depending on the state symmetry.

TABLE IV. Theoretical acceptor energies compared with experiments. Calculations were made for different sets of valence-band parameters μ and δ proposed by several authors.

	Calculated energies (meV)						Observed energies (meV)									
	CdTe	InP		ZnTe			ZnTe:Li			InP:Mg	ZnTe:P			ZnTe:As		
	$\mu=0.69$[a] $\delta=0.12$	$\mu=0.79$[b] $\delta=0.10$	$\mu=0.57$[c] $\delta=0.12$	$\mu=0.61$[d] $\delta=0.15$	$\mu=0.58$[e] $\delta=0.12$	CdTe:Li a	b	f	d	e	f	d	e	f	d
$1S_{3/2}$	54.3	39.5	57.7	51.0	61.5	58.0	40.0	60.5	61.4	61.0	63.5	63.3	63.8	79.0	76.6
$2P_{3/2}$	22.7	17.7	22.2	20.4	23.8	23.9	15.1	22.7	23.8	23.3	23.7	23.7		25.8	23.8
$2S_{3/2}$	15.8	11.8	16.2	14.5	17.3	15.1	11.5	17.1	17.8	17.6	18.5	17.9	18.6	20.2	17.6
$2P_{5/2}(\Gamma_8)$	14.7	11.1	15.1	13.7	16.0	13.6	10.0	16.0	16.6	16.4	17.3	16.8		17.8	15.4
$2P_{5/2}(\Gamma_7)$	11.3	8.3	12.1	10.3	12.9	11.2	7.8	10.4	10.8		10.7	10.3		13.8	11.9
$3S_{3/2}$	8.0	6.1	8.1	7.3	8.6	8.7		7.7	12.2	8.3	9.4	12.7	8.6	12.1	11.5
$4S_{3/2}$	4.9	3.7	4.4	4.4	5.2	5.7		4.6		5.3			5.4	13.5	
$5S_{3/2}$	3.3	2.5	3.8	3.2	4.0	3.4									
$6S_{3/2}$	2.7	1.8	3.2	2.9	3.6			2.9		3.6			3.6		
$7S_{3/2}$	2.3	1.4	2.3	2.1	2.5			1.9		2.6					

[a]Molva *et al.* (Ref. 10).
[b]Barthruff and Haspeklo (Ref. 11).
[c]Venghaus *et al.* (Ref. 13).
[d]Nakashima *et al.* (Ref. 12). We have added globally 3.1 meV to allow for the correction in the energy-gap value used by these authors.
[e]Herbert *et al.* (Ref. 5).
[f]Venghaus and Dean (Ref. 9). These authors assign tentatively 13.8 and 12.1 meV lines to $2p_{5/2}(\Gamma_7)$ and $3S_{3/2}$.

ACKNOWLEDGMENTS

The computer resources were provided by the Centre Inter Regional de Calcul Electronique (Orsay, France) and the Scientific Committee of the Centre de Calcul Vectoriel Pour la Recherche (Palaiseau, France).

APPENDIX: INVERSE POWER METHOD

To partially diagonalize the resulting matrix, we use the Arnoldi method.[8] The principle of this method used to compute the eigenvalues and eigenvectors of a matrix A is the following: One starts with an initial vector v_1 and at every step compute Av_i and orthogonalizes it against all previous vectors to obtain v_{i+1}. At step m, this will build a basis $V_m=\{v_i\}_{i=1,m}$ of the subspace K_m spanned by $V_m=\{v_1, A_1, \ldots, A^{m-1}v_1\}$. By projection onto this basis, the original $n\times n$ matrix A is then reduced to an $m\times m$ matrix, where $m \ll n$. The restriction of A to K_m is represented in basis $\{v_i\}$ by a Hessenberg matrix H_m ($H_m=V_m^T A V_m$). The eigenvalues of H_m will provide approximations to the eigenvalues of A, and eigenvectors z_i of A in K_m are obtained of H_m ones y_i by $z_i=V_m y_i$.

In some cases, the Arnoldi method necessitates more steps to ensure convergence of the process, and this becomes expensive and impractical. In order to avoid the shortcomings of the iterative performance, we use it in conjunction with the inverse power method[18] (Arnoldi inverse power method) that is equivalent to Arnoldi's method applied to the operator $B_+=\mathrm{Re}(A-\sigma I)^{-1}$, where Re stands for the real part of $(A-\sigma I)$ and σ is a complex number that we call shift. It is desirable to work with the shifted and inverted operator B_+ in order to enhance the eigenvalue separation and improve efficiency.

[1]W. Kohn and J. M. Luttinger, Phys. Rev. **98**, 915 (1955).
[2]R. A. Faulkner, Phys. Rev. **184**, 713 (1969).
[3]A. Baldereschi and N. O. Lipari, Phys. Rev. B **8**, 2697 (1973).
[4]A. Baldereschi and N. O. Lipari, Phys. Rev. B **9**, 1525 (1974).
[5]D. C. Herbert, P. J. Dean, H. Venghaus, and J. C. Pfister, J. Phys. C **11**, 3641 (1978).
[6]J. Todd, *A Survey of Numerical Analysis* (McGraw-Hill, New York, 1962).
[7]H. J. Mattausch and Ch. Uihlein, Phys. Status Solidi B **96**, 189 (1979).
[8]Y. Saad, Linear Algebra & Appl. **34**, 269 (1980).
[9]H. Venghaus and P. J. Dean, Phys. Rev. B **21**, 1596 (1980).
[10]F. Morva, J. L. Pautrat, K. Saminadayar, G. Milchberg, and N. Magnea, Phys. Rev. B **30**, 3344 (1984).
[11]D. Barthruff and H. Haspeklo, J. Lumin. **24/25**, 184 (1981).
[12]S. Nakashima, T. Hattori, and P. E. Simmonds, and E. Amzallag, Phys. Rev. B **19**, 3045 (1979).
[13]H. Venghaus, B. Jusserand, and G. Behnke, Solid State Commun. **33**, 371 (1980).
[14]M. Said, M. A. Kanehisa, and M. Jouanne, in Proceedings of the Eighteenth International Conference on the Physics of Semiconductors, Stockholm, 1986 (to be published).
[15]M. Said, M. A. Kanehisa, and M. Balkanski, Solid State Commun. **57**, 417 (1986).
[16]S. Nakashima, H. Kojima, and T. Hattori, Solid State Commun. **17**, 689 (1975).
[17]S. Nakashima (private communication).
[18]B. N. Parlett and Y. Saad, Yale University Research Report YaleU/DCS/RR-424, 1985 (unpublished).